Journal of Vibration Engineering & Technologies (2019) 7:217–226
https://doi.org/10.1007/s42417-019-00114-3

ORIGINAL PAPER

Experimental Investigations: Dynamic Analysis of a Beam Under the Moving Mass to Characterize the Crack Presence

Animesh Chatterjee[1] · **Tanuja Vaidya**[1]

Received: 8 February 2017 / Accepted: 18 November 2017 / Published online: 3 May 2019

Abstract

Background Investigation of the bridge and vehicle interaction problem received an extreme significance due to difficulty of solving the resulted equations, involvement of various parameters such as velocity, mass, traffic intensity, road roughness. The effect of velocity of vehicle on the dynamic response is a key issue in these problems.

Purpose The objective of this study is to evaluate the theoretical results with the experimental results. The displacement and acceleration responses are compared for healthy as well as for damaged beam. A discontinuity present in the response provides the basis for continuous evaluation method for identifying the crack presence and its location.

Methods The problem of dynamic excitation caused by vehicles moving on a bridge is investigated by developing a small scale Lab-model. A beam simply supported is considered as bridge and vehicle is modeled by a moving mass. The mid-span displacement and acceleration response of the simply supported beam are recorded using the CDAQ-card of National Instruments and signal analysis is done with LABVIEW software.

Results It is found that with velocity of mass increasing, vibration amplitude increases but transient fluctuation reduces. A slight shift in the maxima of the response towards right is also observed with increase in velocity. The response is also investigated in presence of crack and it is observed that the amplitude of maxima increases due to crack.

Conclusion The results of experiments are evaluated with simulated theoretical results and it is concluded that presence of crack and its location can be effectively identified using acceleration response. A close estimate is found in the response values of simulated and experimental for the damaged beam subjected to moving mass.

Keywords Small scale model · Bridge and vehicle interaction · Dynamic structural analysis · Dynamic deflection analysis · Dynamic acceleration analysis · Crack identification

Introduction

The field of dynamic interaction of the vehicle with bridge has become a focused area of research due to ever increasing speed of vehicles. Researchers have identified vehicle to bridge mass ratio and vehicle velocity as the two major parameters which largely influence beam response. Among the early research works, an analytical–numerical method was suggested by Akin and Mofid [1] to resolve the governing differential equation of beam over which a mass is traversed. The method converted the partial differential equation into ordinary differential equation. The solutions were compared for various boundary conditions and the significance of consideration of the inertia of the moving mass was explored. Michaltsos et al. [2] used series solution of free vibration of simply supported beam under a moving constant load to obtain dynamic response and investigated the effect of the parameters such as ratio of moving load to beam mass and velocity of moving load.

An approximate and exact approach was attempted by Rahimzadeh and Ali [3] using the Dirac delta function to demonstrate the position of the moving mass and its inertial effect. Results from both the approaches fairly coincide for lower velocities of the moving mass and it was found that the effect of higher vibrational modes cannot be neglected for certain range of velocities. Dehestani et al. [4] developed coupled differential governing equation of the beam

✉ Tanuja Vaidya
tanutagde@gmail.com

Animesh Chatterjee
achatterjee@mec.vnit.ac.in

1 Department of Mechanical Engineering, Visvesvaraya National Institute of Technology, Nagpur, India

using Hamilton's principle for the beam traversed by moving mass with generalized boundary conditions and explored the importance of Coriolis acceleration component for various speeds of the moving mass. Critical influential speed, at which the beam will experience maximum displacement, was studied for various boundary conditions.

Identification of crack in structures is important as it may reduce the life of these structures. Vibration response of the structural members alters with the presence of crack as it introduces local flexibility. This was studied by Chondros et al. [5], who found that the local flexibility introduced by crack reduces the stiffness of the structural members and subsequently its natural frequencies. Dimarogonas [6] presented detailed analytical method to relate the vibration parameters for identifying the crack location and its depth. Experimental data are presented by Bilello et al. [7, 8], which are then compared with the theoretical results based on fracture mechanics approach. Measured response is found to be slightly greater than that obtained analytically. Also, effect of crack is observed to be more on the response than on natural frequency. Stancioiu et al. [9] conducted experiments to analyze the dynamic response of continuous four span beams to the moving mass. The experimental results were found to have reasonable agreement with theoretical values.

Wang and Lee [10] suggested a new sectional flexibility factor for the open single edge crack and demonstrated that for relative crack size less than 0.5, the modified flexibility factor has good conformity with the results of other literature. Pala and Reis [11] showed that the insertion of the centripetal, inertial and Coriolis forces extremely influences the response of the system with increase in speed and mass. Meo et al. [12] have discussed optimum number of sensors and their locations for determining the dynamic response accurately. They used techniques based on maximization of Fisher information matrix and covariance matrix. The method was applied to experiment conducted on Nottingham Wilford suspension bridge. Melcer presented the analysis of dynamic coefficient of a bridge and the dependency of dynamic coefficients of the speed of vehicle motion [13]. A three-dimensional element model was prepared to simulate the bridge and a moving load analysis was performed using the finite element model by Xiao et al. to determine the critical sections of the bridge [14]. Results of a model analysis and field inspections were used to establish a bridge SHM system.

In this paper, a bridge is modeled as a simply supported beam and vehicle as a moving mass. The experimental responses are obtained for healthy and damaged beam and compared with simulated responses based on the velocity of moving mass. Due to presence of crack, the natural frequency of the beam is observed to reduce. The measured displacement response increases due to the crack present in the beam. Also, the measured acceleration response shows the discontinuity which appeared in response curve at the location of the crack is quite supportive in identifying the presence and location of crack.

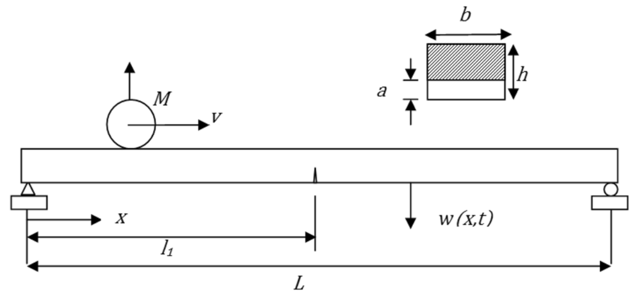

Fig. 1 A cracked simply supported beam under moving mass excitation

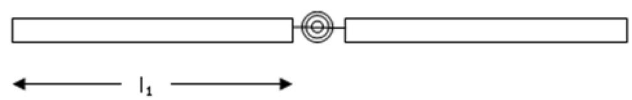

Fig. 2 Model of beam with crack using a torsional spring

Theoretical Analysis and Mathematical Modeling

A cracked simply supported beam is considered as shown in Fig. 1. Parameter a represents crack depth and crack depth ratio is denoted by a/h. l_1 indicates the location of crack from left end of the beam which is located in the middle of span ($l_1 = L/2$). The presence of crack causes the change in local flexibility which is represented by a torsional spring [5] as shown in Fig. 2.

A model is created dividing the beam by a crack into two separate uniform segments connected by a torsional spring having local sectional flexibility at l_1. A parameter c is used to present this flexibility caused due to the crack presence and can be established as [5]:

$$c = \frac{(1 - \vartheta^2)}{\mathrm{EI}} 6\pi h \phi(\alpha), \tag{1}$$

where $\alpha = a/h$ is the crack depth ratio and ϑ is the Poisson ratio.

Using fracture mechanics formulations for a single-sided open crack, we can obtain

$$\phi(\alpha) = 0.655563\alpha^2[0.9566 - 1.5944\alpha + 7.008\alpha^2 - 15.21\alpha^3 + 30.9534\alpha^4 - 50.38657\alpha^5 + 71.8488\alpha^6 - 62.1624\alpha^7 + 29.89486\alpha^{10}]. \quad (2)$$

Deflection response of the cracked beam for each segment can be written as

$$Y_1(x) = C_1\sin(\beta x) + C_2\cos(\beta x) + C_3\sinh(\beta x) + C_4\cosh(\beta x) \quad 0 < x < l_1, \quad (3a)$$

$$Y_2(x) = D_1\sin(\beta(x-l_1)) + D_2\cos(\beta(x-l_1)) + D_3\sinh(\beta(x-l_1)) + D_4\cosh(\beta(x-l_1)) \quad l_1 < x < L. \quad (3b)$$

The applicable boundary conditions are

$$y|_{x=0} = 0, \quad \frac{\partial^2 y}{\partial x^2}|_{x=0} = 0, \quad y|_{x=L} = 0 \quad \text{and} \quad \frac{\partial^2 y}{\partial x^2}|_{x=L} = 0, \quad (4)$$

which gives

$$\begin{bmatrix} \sin(\beta(L-l_1)) & \cos(\beta(L-l_1)) & \sinh(\beta(L-l_1)) & \cosh(\beta(L-l_1)) \\ -\sin(\beta(L-l_1)) & -\cos(\beta(L-l_1)) & \sinh(\beta(L-l_1)) & \cosh(\beta(L-l_1)) \end{bmatrix} \begin{bmatrix} D_1 \\ D_2 \\ D_3 \\ D_4 \end{bmatrix} = \begin{bmatrix} 0 \\ 0 \end{bmatrix}, \quad (5)$$

denoting $y' = \frac{\partial y}{\partial x}$, $y'' = \frac{\partial^2 y}{\partial x^2}$ and $y''' = \frac{\partial^2 y}{\partial x^2}$ and assuming the continuous properties along the beam, the conditions for both segments at the crack location can be written as

$$y_1(l_1,\ t) - y_2(l_1,\ t) = 0, \quad (6a)$$

$$y_1''(l_1,\ t) - y_2''(l_1,\ t) = 0, \quad (6b)$$

$$y_1'''(l_1,\ t) - y_2'''(l_1,\ t) = 0, \quad (6c)$$

$$y_2'(l_1,t)l_1 - y_1'(l_1,t) = y_2''(l_1,t)\left[\frac{(\mathrm{EIc})}{l_1}\right]l_1, \quad (6d)$$

where (EIc/l_1) is the non-dimensional section flexibility of cracked beam.

Equation (6a–6d) along with Eq. (3a) gives

$$\begin{bmatrix} D_1 \\ D_2 \\ D_3 \\ D_4 \end{bmatrix} = \begin{bmatrix} 2a_c - Kb_s & -2b_s - Ka_c & Kb_h & Ka_h \\ 2b_s & 2a_c, & 0 & 0 \\ -Kb_s & -Ka_c & 2a_h + Kb_h & 2b_{hl} + Ka_h \\ 0 & 0 & 2b_h & 2a_h \end{bmatrix} \begin{bmatrix} C_1 \\ C_2 \\ C_3 \\ C_4 \end{bmatrix}, \quad (7)$$

where $K = \beta\mathrm{EIc}$, $a_c = \cos(\beta l_1)$, $a_h = \cosh(\beta l_1)$, $b_s = \sin(\beta l_1)$, $b_h = \sinh(\beta l_1)$, $a_{cl} = \cos(\beta(L-l_1)), a_{hl} = \cosh(\beta(L-l_1))$, $b_{sl} = \sin(\beta(L-l_1)), b_{hl} = \sinh(\beta(L-l_1))$.

Now putting Eq. (7) into Eq. (5) gives

$$\begin{bmatrix} b_{sl} & a_{cl} & b_{hl} & a_{hl} \\ -b_{sl} & -a_{cl} & b_{hl} & a_{hl} \end{bmatrix} \begin{bmatrix} 2a_c - Kb_s & -2b_s - Ka_c & Kb_h & Ka_h \\ 2b_s & 2a_c & 0 & 0 \\ -Kb_s & -Ka_c & 2a_h + Kb_h & 2b_{hl} + Ka_h \\ 0 & 0 & 2b_h & 2a_h \end{bmatrix} \begin{bmatrix} C_1 \\ C_2 \\ C_3 \\ C_4 \end{bmatrix} = \begin{bmatrix} 0 \\ 0 \end{bmatrix}. \quad (8)$$

This result in

$$\begin{bmatrix} b_{sl}N3 + 2b_s a_{cl} - Kb_s b_{hl} & b_{sl}N4 + 2a_c a_{cl} - Ka_c b_{hl} & Kb_h b_{sl} + N1 & Ka_h b_{sl} + N2 \\ -b_{sl}N3 - 2b_s a_{cl} - Kb_s b_{hl} & -b_{sl}N4 - 2a_c a_{cl} - Ka_c b_{hl} & -Kb_h b_{sl} + N1 & -Ka_h b_{sl} + N2 \end{bmatrix} \begin{bmatrix} C_1 \\ 0 \\ C_3 \\ 0 \end{bmatrix} = \begin{bmatrix} 0 \\ 0 \end{bmatrix}, \quad (9)$$

where the constants are $N1 = (2a_h + Kb_h)b_{hl} + 2b_h a_{hl}$; $N2 = b_{hl}(2b_{hl} + Ka_h) + 2a_h a_{hl}$; $N3 = (2a_c - Kb_s)$; $N4 = (-2b_s - Ka_c)$.

For non-trivial solution of Eq. (9) to exit, the coefficient determinant needs to be equal to zero which gives the required frequency equation as

$$\begin{aligned}
&2\cos(l_1\beta)\cosh(l_1\beta)\sin((L-l_1)\beta)\sinh((L-l_1)\beta)\\
&+2\cos((L-l_1)\beta)\cosh(l_1\beta)\sin(l_1\beta)\sinh((L-l_1)\beta)\\
&-K\cosh(l_1\beta)\sin((L-l_1)\beta)\sin(l_1\beta)\sinh((L-l_1)\beta)\\
&+2\cos(l_1\beta)\cosh((L-l_1)\beta)\sin((L-l_1)\beta)\sinh(l_1\beta)\\
&+2\cos((L-l_1)\beta)\cosh((L-l_1)\beta)\sin(l_1\beta)\sinh(l_1\beta)\\
&-K\cosh((L-l_1)\beta)\sin((L-l_1)\beta)\sin\left(l_1\beta\right)\sinh\left(l_1\beta\right)\\
&+K\cos\left(l_1\beta\right)\sin\left(\left(L-l_1\right)\beta\right)\sinh((L-l_1)\beta)\sinh(l_1\beta)\\
&+K\cos((L-l_1)\beta)\sin(l_1\beta)\sinh((L-l_1)\beta)\sinh(l_1\beta)=0.
\end{aligned} \tag{10}$$

After solving this determinant, multiple values of β, i.e. non-dimensional natural frequency can be obtained. The value of the C_3 is found by inserting the value of β in Eq. (9). Then the mode shapes of the damaged beam are found and used to found the vibration response of damaged beam.

Mathematical model for the moving mass problem is based on following assumptions:

1. Damping is negligible in the system.
2. Rotary inertia and shear force effects in the beam are neglected.
3. The moving mass is traversing with constant velocity.
4. The beam is having constant mass density and symmetric section along the length.
5. Boundary conditions are considered as simply supported at both the ends.
6. Moving vehicle is considered as a rigid mass and it is always in contact with the beam.

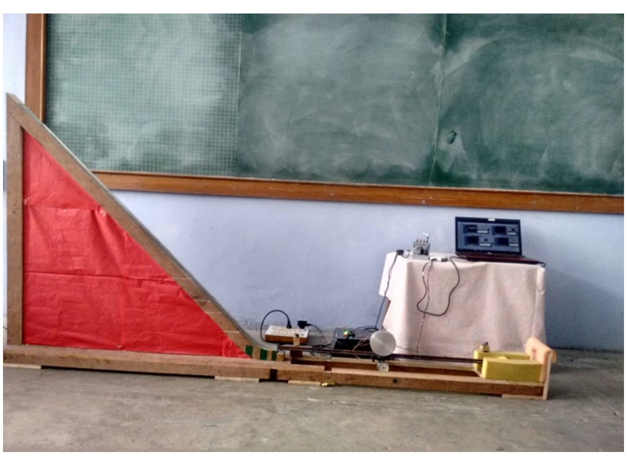

Fig. 3 Experimental setup

Based on the above assumptions, the governing equation of motion of the Euler–Bernoulli simply supported beam under the moving mass can be written as [11, 15]:

$$\mathrm{EI}\frac{\partial^4 y(x,t)}{\partial x^4} + \rho A\frac{\partial^2 y(x,t)}{\partial t^2} = \left[Mg - M\frac{\mathrm{d}^2 y(vt,t)}{\mathrm{d}t^2}\right]\delta(x-vt), \tag{11}$$

where E is elastic modulus of the beam material, ρ is the mass density of the beam, $y(x, t)$ is the dynamic deflection, A is the area and I is second moment of area of the beam cross section. M is mass, v is velocity of the vehicle and $\delta\,(x-ut)$ is the delayed Dirac delta impulse function. Using the mode superposition principle

$$y(x,t) = \sum_{n=1}^{N} Y_n(x)\cdot q_n(t), \tag{12}$$

Equation (11) can be written as

$$\begin{aligned}
&\sum_{n=1}^{\infty}\omega_n^2\rho A Y_n(x)q_n(t) + \sum_{n=1}^{\infty}\rho A\frac{\mathrm{d}^2 q_n(t)}{\mathrm{d}t^2}Y_n(x)\\
&+M\left[\sum_{n=1}^{\infty}\frac{\mathrm{d}^2 q_n(t)}{\mathrm{d}t^2}Y_n(x) + \sum_{n=1}^{\infty}2v\frac{\mathrm{d}Y_n(x)}{\mathrm{d}x}\frac{\mathrm{d}q_n(t)}{\mathrm{d}t}Y_n(x)\right.\\
&\left.+\sum_{n=1}^{\infty}v^2\frac{\mathrm{d}^2 Y_n(x)}{\mathrm{d}x^2}q_n(t)\right]\delta(x-vt) = Mg\delta(x-vt).
\end{aligned} \tag{13}$$

The equation is then multiplied with another mode and integrated over the domain. Using the Dirac delta properties and orthogonality properties, the equation is simplified as

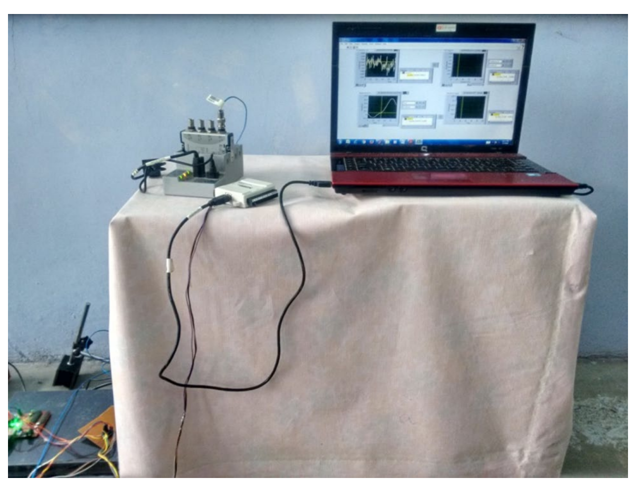

Fig. 4 CDAQ-9174 and DAQ-6009 of NI used with Lab-View software

$$\omega_n^2 q_n(t) + \ddot{q}_n(t) + \frac{2M}{mL}\sum_{j=1}^{\infty} Y_n(x)Y_j(x)\ddot{q}_j(t) + \frac{4Mv}{mL}\sum_{j=1}^{\infty}\frac{j\pi}{L}Y_j'(x)Y_n(x)\dot{q}_j(t) - \frac{2Mv^2}{mL}\sum_{j=1}^{\infty}\left(\frac{j\pi}{L}\right)^2 Y_j''(x)Y_n(x)q_j(t) = \frac{2Mg}{mL}Y_n(x). \tag{14}$$

Mode shape for simply supported damaged beam is used in Eq. (14) and solved using the numerical integration method.

Experimental Analysis

The framework of the experiments conducted is explained in detail. The experiments are carried out for the healthy as well as for damaged beam. The characteristics of the experimental model are shown in Fig. 3, in which the model consists of the steel beam with length $L = 1.016$ m, width, $w = 0.0386$ m, thickness, $t = 0.00525$ m, and $\rho = 7800$ kg/m^3. A steel rail of dimensions $1.02 \times 0.00855 \times 0.00842$ is glued to the middle of beam to guide the movement of the moving mass, which gives EI = 711.5764 N m^2 for the beam and rail combined section. The weight of the beam and rail assembly is 20.699 N.

The beam is simply supported at each end. The left end is supported on the knife edge support which is rested on the wooden block. This wooden block is fixed on the wooden platform. The right end support is supported on a roller which is placed on the wooden platform. The wooden platform is placed on the rigid concrete block. A wooden ramp is placed next to the left end side for providing the speed to the rolling mass prior to entering the beam. A thin layer of aluminum is placed on the ramp to form the rolling surface to which a rail of same dimension (as used on beam) is glued to the ramp. The inclination of the ramp surface is 60° and placed on the rigid concrete block.

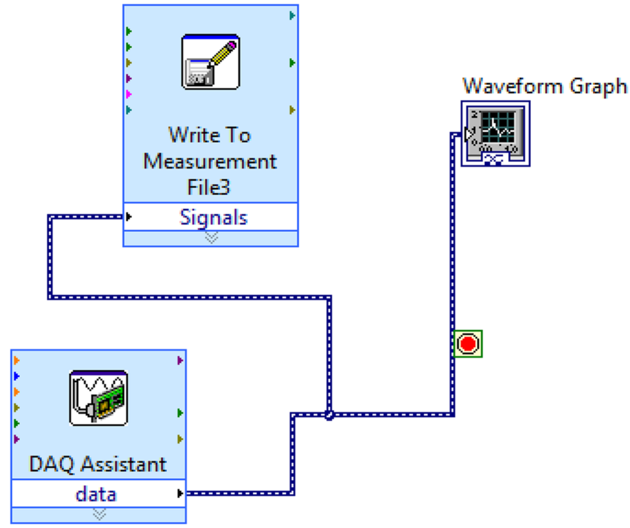

Fig. 6 Lab-View software circuit diagram used for speed measurement

A rolling mass of aluminum is pre-machined to have a center diametrical notch so that it could roll over the beam freely. The size of notch drilled into the rolling mass is 0.0095×0.01016 m. The diameter and thickness of the rolling mass are 0.12098 m and 0.040259 m, respectively. The total weight of the rolling mass measured is 11.18 N.

An ICP accelerometer (make: PCB) with sensitivity of 100 mV/g and frequency range of 0.5–10 kHz is used to acquire the vibration signals. An accelerometer with magnetic base was attached to the middle of the beam from the bottom side. The vibration signals are taken from the accelerometer to the LabVIEW software through the CDAQ-card 9174 of National Instruments. A LabVIEW circuit diagram used to obtain the signal is shown in Fig. 4. The data obtained are then re-plotted in MATLAB.

For the speed measurement of the rolling mass, two infrared-based sensors (TSOP sensor module) with a specific

Fig. 5 Circuit connections for the speed measurement

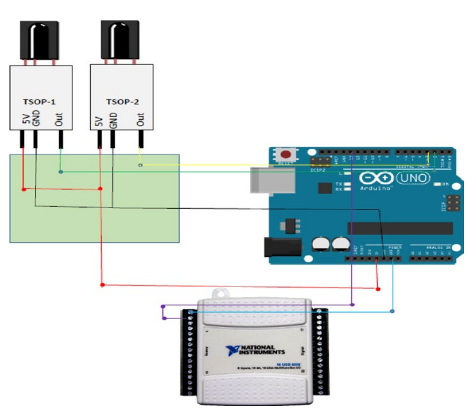

Connections

a) 5V & GND from TSOP1

b) & TSOP2 to 5V of ARDUINO

c) OUT from TSOP1 to digital pin 2

d) OUT from TSOP2 to digital pin 3

e) Digital pin 3 to AI0 of USB-6009 DAQ-card

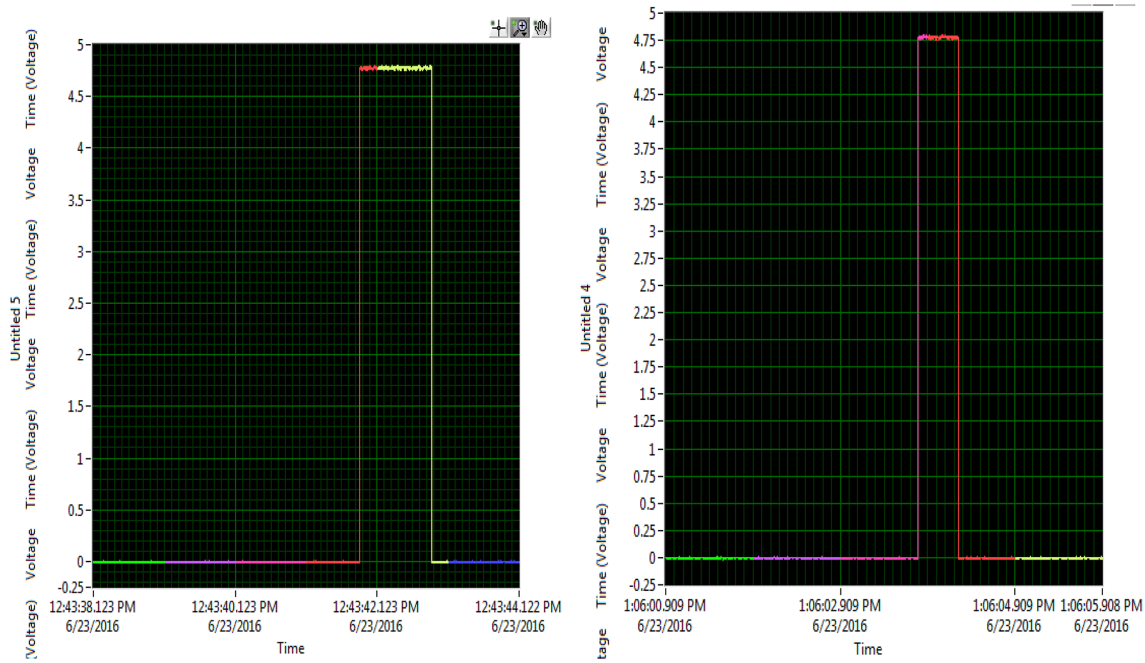

(a) V=1m/s; V/Vcr=0.022 **(b)** V=2m/s; V/Vcr=0.044

Fig. 7 Volt signal generated by IR sensor for speed measurement

frequency of *38* kHz supported through the Arduino micro-controller board are placed facing the entry and exit points of the rolling mass over the beam. The Arduino is connected to the USB-6009 DAQ-card 6009 by National Instruments.

Speed Measurement of the Rolling Mass

The details of configuration and working principle of the whole circuit designed to measure the speed of the rolling mass are presented. The speed measurement of the rolling mass is done by detecting the arrival and exit times of the rolling mass on the beam. The whole circuit is then integrated with USB-6009 DAQ-card of NI to acquire the data.

All the components used in the circuit, i.e., TSOP sensors, Arduino Board and NI USB-6009, are connected for the speed measurement as shown in Fig. 5, in which Arduino program is dumped to the Arduino board through the Arduino IDE. The measurements are conducted for two velocities of the moving mass which include 1 m/s and 2 m/s. The height for providing the velocity to the rolling mass is calculated theoretically and marked on the ramp so that the moving mass could acquire the velocity expected. The LabVIEW circuit as shown in Fig. 6 is designed to obtain and save the measured data for speed measurement.

Figure 7a, b shows that measured speed of moving mass is confirmed with the speed expected for which theoretical height was estimated. A volt signal of around 5 V is generated at the entry of the moving mass on the beam

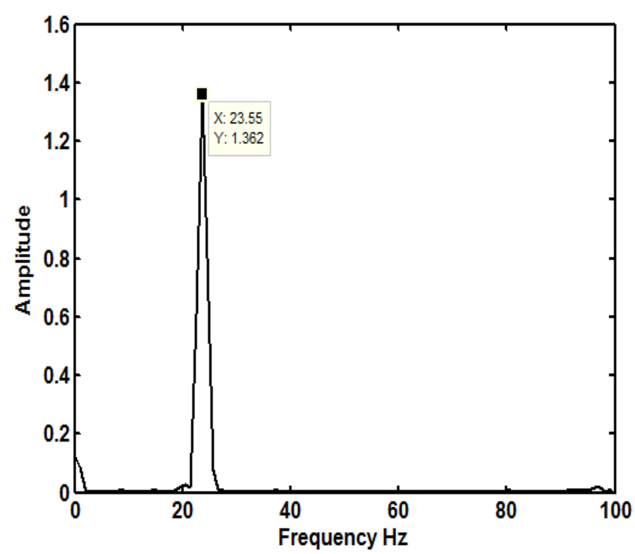

Fig. 8 FFT of acceleration response

which continues till the moving mass exits. The velocity is estimated from the time taken by the moving mass to traverse the beam of length 1 m. Figure 7a shows that the mass traversed over the beam with a velocity of 1 m/s as the time taken is 1 s, while Fig. 7b shows that it is 2 m/s as the time taken is 0.5 s.

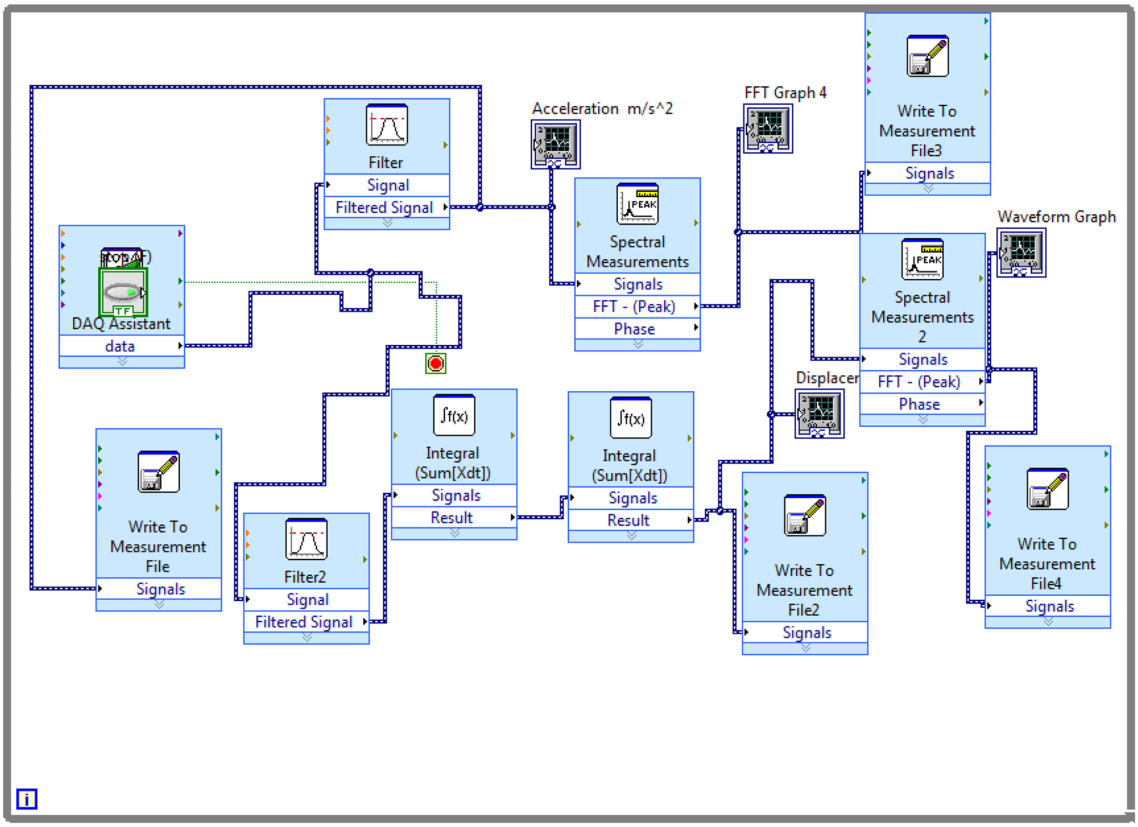

Fig. 9 Lab-View circuit diagram for the response measurement

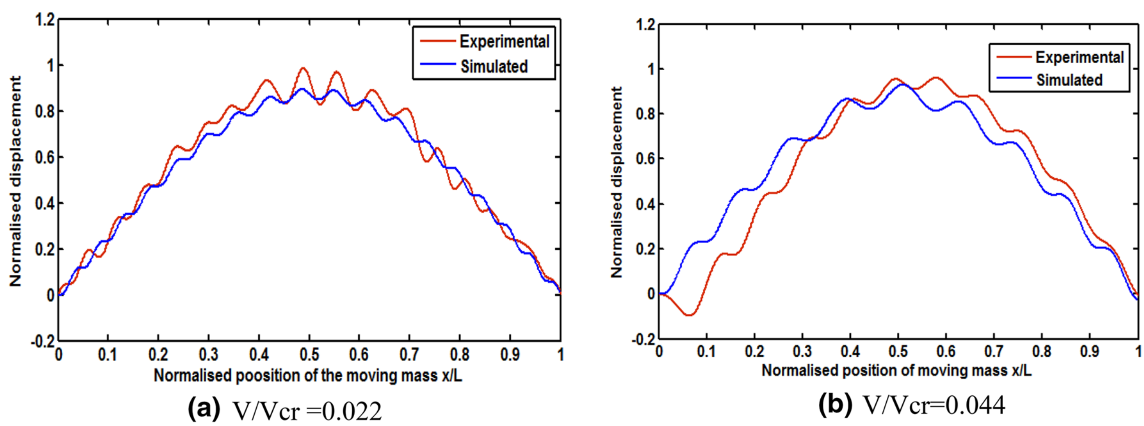

Fig. 10 Simulated and experimental displacement response of healthy beam

Methodology of Experiment

Initially, the maximum static deflection of the beam is measured to estimate the natural frequency theoretically. A natural frequency of the beam is taken by LabVIEW through FFT from the free vibration analysis. Both the frequencies are compared. A moving mass is first rolled over the beam from the height corresponding to the speed of 1 m/s. The acceleration response, displacement response and the FFT of both the responses are recorded. A bandpass finite impulse response filter is applied to the acceleration signal while bandpass Butterworth infinite impulse response filter is applied to the displacement signal. The same sequence of experiment is conducted for the velocity 2 m/s and on the damaged beam. A crack of relative size 0.25 is induced in the beam near the mid-span of the beam. The crack size was

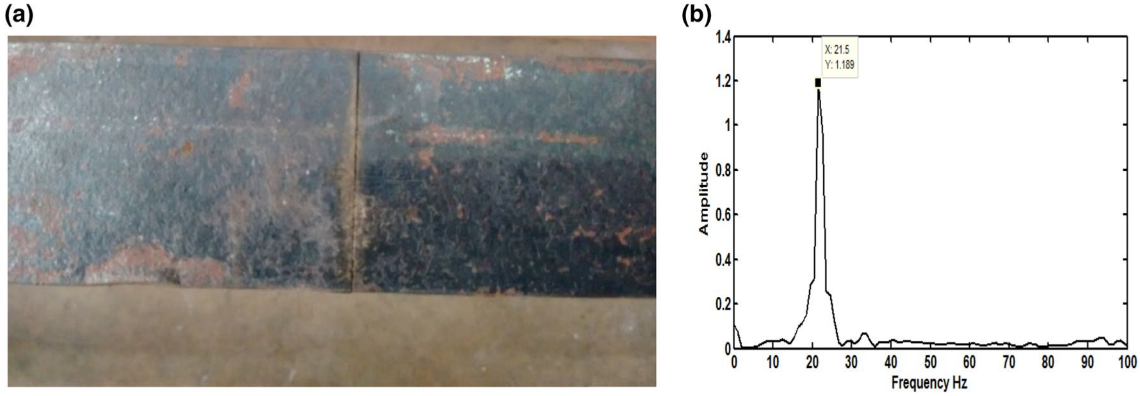

Fig. 11 **a** A crack introduced in the beam near the middle of the beam; **b** FFT of acceleration response of cracked beam

selected on the basis of previous research work by Pala and Reis [11], who have considered crack size between 0.25 and 0.75 and Mahmoud and Zaid [16], who considered crack size between 0.2 and 0.6.

Results and Discussion

Initially, the measurements are taken to estimate the natural frequency of the beam by calculating the bending stiffness of the beam and rail assembly from the static loading. A maximum static deflection of the beam rail assembly is measured by the dial gauge.

The measured maximum static deflection of the beam resulted as

$$Y_{\text{static-max}} = 0.56\ \text{mm}.$$

Therefore, the bending stiffness of the beam and rail assembly can be calculated as

$$Y_{\text{static-max}} = \frac{WL^3}{48\text{EI}}, \tag{15}$$

$$0.56 \times 10^{-3} = \frac{1.14 \times 9.81 \times (1)^3}{48\text{EI}}, \tag{16}$$

$$\text{EI} = 436.3407\ \text{N\_m}^2,$$

$$\omega = \left(\frac{n\pi}{L}\right)^2 \times \sqrt{\frac{\text{EI}}{\rho A}}, \tag{17}$$

$$\omega_1 = \left(\frac{1 \times \pi}{0.97}\right)^2 \times \sqrt{\frac{436.3407}{2.11}}, \tag{18}$$

$$\omega_1 = 147.78\ \text{rad/s};\ f_1 = 23.52\ \text{Hz}.$$

FFT of the response of the beam and rail assembly is taken in LabVIEW through the free vibration analysis as shown in Fig. 8 which shows the natural frequency $f_1 = 23.55$ Hz. Therefore, the critical velocity obtained is $V_{cr} = 45.59$ m/s. The natural frequency obtained by static deflection measurement is slightly lesser than obtained from free vibration response. The LabVIEW circuit used to record the measurements is shown in Fig. 9.

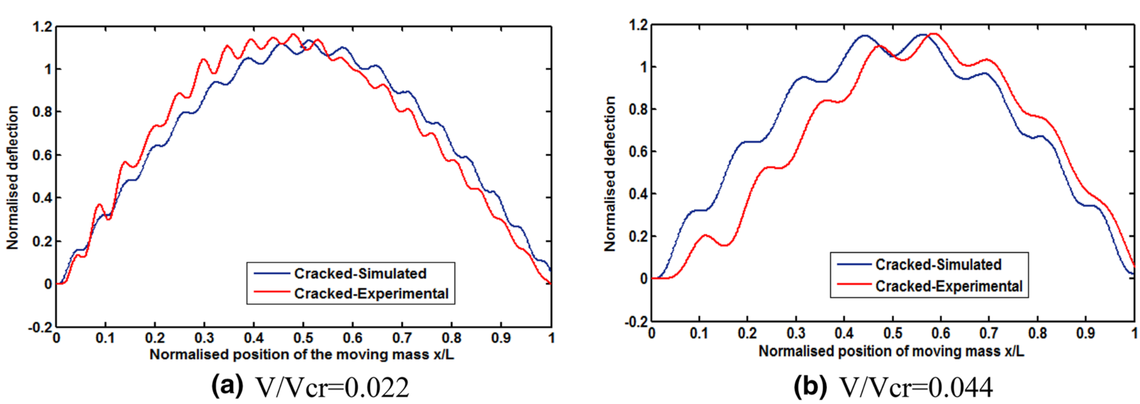

Fig. 12 Comparison of simulated and experimental displacement response of cracked beam ($\alpha = 0.25$, $l_1 = 0.478$ L)

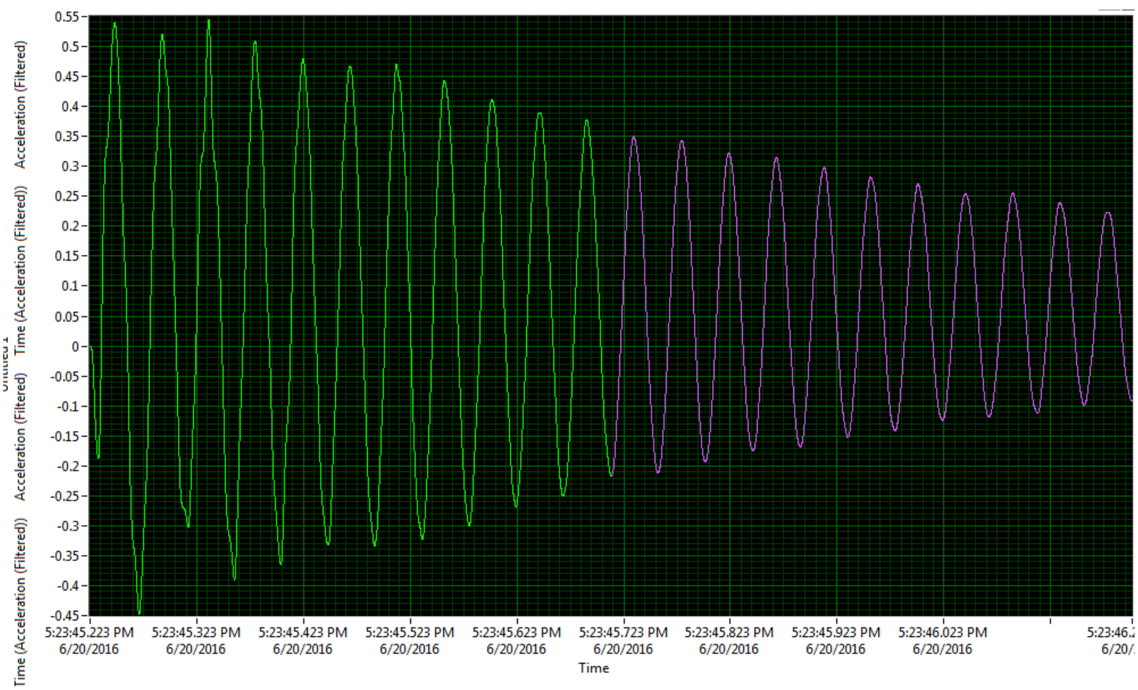

(a) Healthy beam

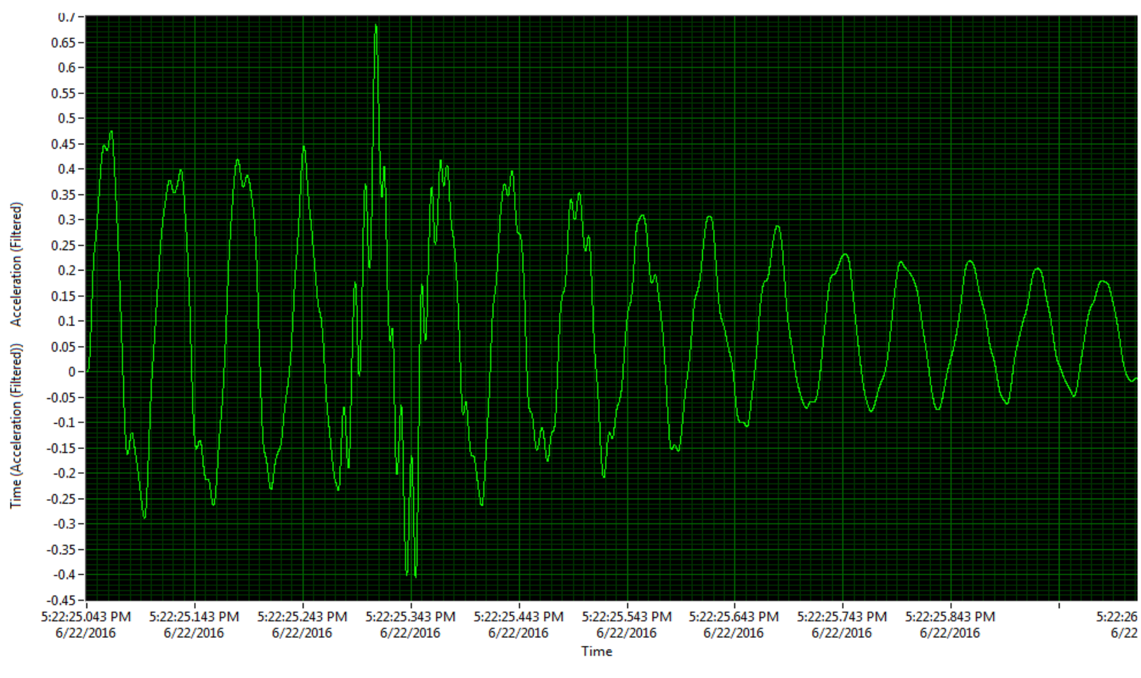

(b) Cracked beam

Fig. 13 Acceleration response of the beam for velocity ratio $V/V_{cr}=0.044$

The displacement response obtained from the experiment is compared with that of simulated in the MATLAB shown in Fig. 10. A half sine curve is obtained with the number of oscillations present in the response. Also a curve is symmetric about the middle of beam. The profile and trend of the displacement curve is similar to that obtained theoretically.

The number of oscillations is also nearly the same with that present in the simulated response. Though the maximum value of experimental displacement is slightly higher but a good correlation in the values of displacement of experimental response and simulated one is obtained.

Then a crack is introduced in the beam of relative size $\alpha = 0.25$ at the location 0.487 L from the left end as shown in Fig. 11a. The natural frequency of the cracked beam is theoretically calculated with reference to Eq. (10). The calculated first natural frequency of the cracked beam is $f_1 = 21.3967$ Hz. Now, a maximum static deflection of cracked beam is measured with dial gauge, from which a natural frequency is determined as follows:

$$Y_{\text{static-max}} = 0.66 \text{ mm}.$$

Therefore, the bending stiffness of the beam and rail assembly is found as

$$\text{EI} = 353 \text{ N\_m}^2,$$

$$\omega = \left(\frac{n\pi}{L}\right)^2 \times \sqrt{\frac{\text{EI}}{\rho A}}, \tag{19}$$

$$\omega_1 = 135.67 \text{ rad/s}; \quad f_1 = 21.59 \text{ Hz}.$$

Natural frequency shown by FFT (Fig. 11b) through the free and forced vibration analyses is slightly lesser, i.e., $f_1 = 21.5$ Hz than that is calculated by static deflection. The characteristics which include the profile of response, trend, and oscillations are found to be similar in experimental displacement response with that of the simulated response. The experimental displacement value is slightly higher than it is for simulated as shown in Fig. 12. Also, the response is not symmetric about the middle of the beam. The acceleration response of healthy and damaged beam for velocity ratio 0.044 can be observed in Fig. 13. A discontinuity is evident at the crack location in the acceleration signal of damaged beam while it is a smooth curve in case of healthy beam.

Conclusion

A series of experiments are carried out for presenting the dynamic response of the healthy as well as damaged beam subjected to the moving mass excitation. Natural frequency of the rail and beam assembly is found from the static deflection and also from the free vibration analysis. Both the frequencies are found to be same. A good correlation is obtained in the dynamic response of the simulated and experimental. A similarity is found in terms of profile of curve, oscillations, and trend. Experimental displacement values are found to be slightly higher compared to that of simulated. After initiating a crack in beam, again a natural frequency is obtained by measuring the maximum static deflection and from the free vibration analysis. Increase in response is obtained due to the presence of crack. A close estimate is found in the response values of simulated and experimental for the damaged beam subjected to moving mass. A simulated response is symmetric about the middle of beam while it is shifted due to the presence of crack. A discontinuity appeared in the acceleration response of the damaged beam at the location of the crack. So, the presence of crack could be predicted with the help of the acceleration response.

References

1. Akin JE, Mofid M (1989) Numerical solution for response of beams with moving mass. J Struct Eng 115(1):120–131
2. Michaltsos G, Sophianopoulos D, Kounadis AN (1996) The effect of moving mass and other parameters on the dynamic response of a simply supported beam. J Sound Vib 191(3):357–362
3. Rahimzadeh RF, Ali N (2008) Dynamic behavior and modal control of Euler-Bernoulli beams under moving mass. J Appl Math 1:293–304
4. Dehestani M, Mofid M, Vafai A (2009) Investigation of critical influential speed for moving mass problems on beams. App Math Model 33:3885–3895
5. Chondros TG, Dimarogonas AD, Yao J (1998) A continuous cracked beam vibration theory. J Sound Vib 215(1):17–34
6. Dimarogonas AD (1996) Vibration of cracked structures: a state of the art review. Eng Fract Mech 55(5):831–857
7. Bilello C, Bergman LA (2003) Vibration of damaged beams under a moving mass: theory and experimental validation. J Sound Vib. https://doi.org/10.1016/j.jsv.2003.01.001
8. Bilello C, Bergman LA, Kuchma D (2004) Experimental investigation of a small-scale bridge model under a moving mass. J Struct Eng 130(5):799–804
9. Stancioiu D, James S, Ouyang H, Mottershead JE (2009) Vibration of a continuous beam excited by a moving mass and experimental validation. 7th international conference on modern practice in stress and vibration analysis. J Phys Conf Ser 181:012084
10. Wang C-S, Lee L-T (2012) Modified and simplified sectional flexibility of a cracked beam. J Appl Math 2012, Article ID 543828
11. Pala Y, Reis M (2012) Dynamic response of a cracked beam under a moving mass load. J Eng Mech 1:1. https://doi.org/10.1061/(ASCE)EM.1943-7889.0000558
12. Meo M, Zumpano G, Meng X, Cosser E, Roberts G, Dodson A (2006) Measurements of dynamic properties of a medium span suspension bridge by using the wavelet transforms. Mech Syst Signal Process 20:1112–1133
13. Melcer J (2015) Dynamic response of a bridge due to moving loads. J Vib Eng Technol 3(2):199–209
14. Xiao F, Leroyhulsey J, Chen G (2016) Structural health monitoring of the Klehini river bridge. J Vib Eng Technol 4(4):309–318
15. Vaidya T, Chatterjee A (2017) Vibration of road bridges under moving vehicles: a comparative study between single contact point and two contact point models. Trans Can Soc Mech Eng 41(1):99–111
16. Mahmoud MA, Zaid MA (2002) Dynamic response of a beam with a crack subject to a moving mass. J Sound Vib 256(4):591–603